Applied Thermal Engineering 144 (2018) 392–402

Contents lists available at ScienceDirect

Applied Thermal Engineering

journal homepage: www.elsevier.com/locate/apthermeng

Research Paper

The performance and risk assessment of R290 in a 13 kW air source heat pump

Weier Tang[a], Guogeng He[a,*], Sai Zhou[a], Wei Sun[a], Dehua Cai[a], Kui Mei[b]

[a] School of Energy and Power Engineering, Huazhong University of Science and Technology, Wuhan 430074, China
[b] Nanjing TICA Climate Solutions Co., Ltd, Nanjing, China

HIGHLIGHTS

- Performance of R290 in a 5P ASHP was measured.
- Experimental study on the risk after a R290 leakage from the ASHP was first presented.
- R290 concentration distribution in the surrounding area of ASHP was detected.
- R290 concentration in the electric control cabinet of ASHP was explored for the first time.
- Some safety measures to minimize the risk of R290 ASHP were proposed.

ARTICLE INFO

Keywords:
R290
Heat pump
Performance
Leakage
Concentration distribution

ABSTRACT

Currently, with the growing concerns about global climate change, R290 has been considered as a competitive next generation refrigerant used in the air source heat pump (ASHP). However, the flammable characteristics of R290 prevented its wide application in the large ASHP system. This paper mainly contributed to the application of R290 in an ASHP with a nominal heating capacity of 13 kW. Firstly, the performance of R290 in the ASHP was measured. By optimizing the equipment of the refrigeration system, the charge of R290 in this ASHP is reduced to 1.3 kg which meet the requirements of the EN378-1 (2016), and the coefficient of performance (COP) of this R290 ASHP could reach 2.8 and 3.27 respectively in the rated refrigerating and heating conditions, which could meet the corresponding Chinese national standards. Then the experimental investigation on the risk after a R290 leakage from the ASHP was presented for the first time. The R290 concentration distribution in the ASHP surrounding and internal area was measured when the leakage occurred in different scenarios. The results showed that the combustible zone will continuously appear in the inside area of the ASHP during the whole leakage process. But in the outside area, it only appeared in the region where around the ASHP and extremely close to the ground. Finally, some suggestions according to the experimental results were presented to improve the safety design of the R290 ASHP.

1. Introduction

Air source heat pump (ASHP) has many advantages on thermal conversion efficiency, energy conservation and environment protection [1]. However, the refrigerants deployed in conventional ASHP is harmful to the environment. R22 is on the phase-out list with the hydrochlorofluorocarbons (HCFCs) according to the Montreal Protocol due to its high ODP (ozone depletion potential) effects [2]. R134a and R410a emerged several years ago as the potential replacement to R22 in ASHP, but these hydrofluorocarbons (HFCs) have a relatively high GWP (global warming potential) values, the emissions of them contributed to the more global release of carbon dioxide equivalents [3]. In October 2016, more than 170 countries agreed on the Kigali Amendment, which pointed out that the use of the HFCs will be phased down in the coming decades [4]. Hence, it is urgent to find the next generation refrigerant with low climate effect in the ASHP. The natural refrigerant R290 has been expected as one of the promising and competitive candidates.

The environmental characteristics of zero ODP and very low GWP values make R290 has attracted the worldwide attention, several studies about R290 in heat pump have been carried out in the past. For example, Blanco et al. [5] evaluated the performance of an air-to-water at different superheat conditions using R290 as the refrigerant. Chang

* Corresponding author.
E-mail address: gghe@mail.hust.edu.cn (G. He).

https://doi.org/10.1016/j.applthermaleng.2018.08.070
Received 12 April 2018; Received in revised form 5 July 2018; Accepted 19 August 2018
Available online 20 August 2018
1359-4311/ © 2018 Elsevier Ltd. All rights reserved.

Nomenclature

ASHP	air source heat pump
COP	coefficient of performance
ECC	electric control cabinet
GWP	global warming potential
HCFC	hydrochlorofluorocarbon
HFC	hydrofluorocarbon
LFL	lower flammable limit
ODP	ozone depletion potential
UFL	upper flammable limit
C_p	specific heat capacity of water (KJ/kg·°C)
M_w	mass flow rate of water (kg/s)
Q	heating/cooling capacity (kW)
T_{in}	inlet temperature of the water (°C)
T_{out}	outlet temperature of the water (°C)
W	power consumption of the scroll compressor (kW)

et al. [6] found the cooling and heating capacities of R290 in heat pump are slightly smaller than R22 but the coefficient of performance (COP) is slightly higher. Nawaz et al. [7] developed a component-based model which calibrated by the experimental data to predict the performance of R290 in the heat pump water heater system. Fernando et al. [8] proposed a method of using mini-channel heat exchangers to reduce the R290 charge amount in heat pump without the loss of COP. Ghoubali et al. [9] reviewed the standards on R290 in heat pump and presented a COP optimization study on the R290 heat pump with three different types of condensers. These literatures indicated that comparing the current refrigerants in the heat pump, R290 has the advantages in thermodynamic performance, economic efficiency, and environmental characteristics. However, the wide application of R290 in heat pump was prevented by its flammable characteristics. The lower minimum ignition energy of R290 is only 0.48 mJ at a concentration of 5.2 vol% [10], and the lower and upper flammable limits (LFL and UFL) of R290 in the air at 25 °C and 1 atm is at a very low concentration of 2.1 and 9.5 vol% [11], respectively. Therefore, it was classed as an A3 flammable refrigerant by ASHRAE, and the maximum charge quantity of R290 in refrigerant equipment is strictly restricted by the international criterions, i.e., EN 378, ISO 5149 and IEC 60335-2-40 [12]. The special precautions are needed in the use of R290.

Many studies have concerned the safety of R290 or other flammable refrigerants on refrigerant equipment. The quantitative risk assessment (QRA) model was proposed by Colbourne and Suen [13] to appraise the potential for ignition when hydrocarbons leaked from refrigerant equipment, and was used to evaluate the flammability risk of R290 in ice cream cabinet [14], split air conditioner and refrigerator [15]. Gigiel [16] carried out the safety test of domestic refrigerators with flammable refrigerants according to the methods specified in the safety standard, IEC/EN 60335-2-24. Jia et al. [17] analyzed the leakage and diffusion of R32 of a wall-mounted air conditioner and discuss the impact of air velocity and leakage hole position on the R32 indoor concentration distribution. Li [18] measured the R290 distribution inside a room under different scenarios and explored the influence of leak rate, leak point location and indoor fan. Zhang et al. [19] evaluated the overpressure arising and total heat release rate from an external fire imposed upon an R290 air-conditioner and investigated the explosion characteristics through the R290 air conditioner deflagration experiments [20].

From these previous studies, it could be known that due to the limitation of the R290 charge quantity, the performance of the R290 heat pump was usually carried out under the condition that the R290 charge quantity is less than 1.0 kg. Besides, the studies of R290 safety were mainly focused on the air conditioners or refrigerators, there is a little information available in the current literatures about the R290 risk in the heat pump. With the widespread application of heat pump in residential and commercial facilities and the acceleration of the phase-out process of HCFCs and HFCs, the performance and risk of the R290 heat pump with a large refrigerant charge quantity still need further research. In this paper, the performance of an R290 ASHP with a nominal heating capacity of 13 kW was measured and compared under different environmental conditions. Then the potential fire hazards around the R290 ASHP and inside the electric control cabinet (ECC) were evaluated through the R290 leakage under different scenarios. The influence of ASHP location and the height of leak position on the risk will be discussed. The results could provide powerful support to improve the design of R290 ASHP and minimize the risks of using R290 in ASHP.

2. Performance experiment of the R290 ASHP

2.1. The equipment optimization of the system

In this study, an R290 ASHP (850 (L) ×480 (W) ×1755(H) mm) with a nominal heating capacity of 13 kW was employed in the experiments. The prototype of this ASHP applied R22 as refrigerant while the diameter of the tube of the air-to-refrigerant heat exchanger is 9.52 mm, and the total numbers of tubes are 84. The compressor was replaced by a special R290 hermetic scroll compressor with 17.1 m^3/h displacement, which specially developed for R290 by Emerson, to use R290 as working fluid in this ASHP system. Besides, the R290 ASHP needs to take some technical measures to reduce the refrigerant charge amount to minimize the potential risk associated with a sudden leakage of the flammable refrigerant, many researchers have presented their studies about the charge reduction in the R290 heat pump system [21–23]. IIR [24] also has provided some recommendations for charge reduction in the refrigeration system, and the main design guideline is the minimization of the internal volume of the components, especially the components which contain the liquid refrigerant. The reason is that if these components have a large internal volume, they will have a higher capability to store the extra refrigerant in it with liquid form, which will make the refrigerant charge in the system higher. Hence, a high efficiency brazed plate-type heat exchanger was employed on the refrigerant-to-water side, the internal volume of the refrigerant side is only about 0.6×10^{-3} m^3. The heat transfer capacity of this plate-type heat exchanger is 15.17 kW since the heat transfer area is 0.97 m^2, the mean temperature difference is 5.0 °C and the overall heat transfer coefficient is 3128 W/(°C*m^2).

Besides, on the air-to-refrigerant side, the smaller diameter tubes were considered to reduce the internal volume. Comparing with R22, the saturated liquid density of R290 is lower, but the heat transfer coefficient is higher in the same system cooling capacity and diameter of the tube [25]. These thermodynamic properties make it possible to use a smaller diameter of heat exchanger tube to reduce the R290 charge quantity, which has been successfully applied in the air conditioner [26,27]. The air-to-refrigerant heat exchanger was therefore redesigned and the diameter of the tube of the air-to-refrigerant heat exchanger was reduced from 9.52 mm to 7.0 mm. However, the smaller diameter tends to bring a high-pressure drop inside the tube, which need to compensate by reducing the refrigerant circulation velocity through increasing the number of tubes. Hence, the total number of tubes in the air-to-refrigerant heat exchanger was increased from 84 to 96 and the internal volume was reduced from 6.7×10^{-3} m^3 to 4.2×10^{-3} m^3. In this new small tube air-to-refrigerant heat exchanger, the heat transfer area of the air side is 50.4 m^2, the designed logarithmic mean temperature difference is 8.5 °C, the heat transfer coefficient of the fin side is according to 42 W/(°C m^2). As a result, the

heat transfer capacity of this air-to-refrigerant heat exchanger is 17.99 kW, which could meet the system requirements. The specifications of the apparatus parameters in the ASHP were shown in Table 1.

2.2. Performance measurement of the ASHP

The experiment is conducted in the heat pump testing lab (Fig. 1), of which the schematic diagram is shown in Fig. 2. For measuring the cooling/heating capacity, two platinum resistances were utilized to measure the inlet and outlet temperature of the water-side, then by measuring the mass flow rate of water through the flowmeter, the cooling/heating capacity could be calculated by the Eq. (1):

$$Q = C_p \times M_w \times (T_{out} - T_{in}) \quad (1)$$

where Q is the cooling/heating capacity (kW); C_p is the specific heat capacity of water (KJ/kg·°C); M_w is the mass flow rate of water (kg/s); T_{out} and T_{in} is the outlet and inlet temperature of the water (°C).

In order to obtain the refrigeration cycle characteristics with regard to temperature, a series of T type thermocouples are pasted on the copper tubes at different locations, including the inlet, outlet and middle of different pipe paths of the heat exchangers. The wattmeter was employed to measure the power of the scroll compressor, and experimental apparatus specifications were shown in Table 2. The COP in the system could be calculated by the Eq. (2):

$$COP = \frac{Q}{W} \quad (2)$$

where W is the power consumption of the scroll compressor (kW).

The results of the performance experiment under rated refrigerating and heating condition were shown in Table 3. As shown in Fig. 2, an accumulator was used in this system to store the excess refrigerant in heating mode. In the beginning, the inner volume of this accumulator is 2.5×10^{-3} m^3, the optimal R290 charge quantity in this situation is 1.8 kg, and the COP of rated refrigerating and heating mode is 2.62 and 3.25, respectively. However, according to the EN378-1 (2016), this ASHP belongs to the indirect closed system and general occupation category, the maximum R290 charge quantity is restricted to 1.5 kg. Therefore, the 1.8 kg R290 charge quantity does not conform to the regulations of EN 378, it needs to take some measures to further reduce the R290 charge quantity. From the recommendations of IIR [24], the internal volume of the components which contain the liquid refrigerant should be minimized. Since the diameter of air-to-refrigerant heat exchanger tube has been reduced from 9.52 mm to 7, the inner volume reduction of the accumulator was considered. The accumulator will store the extra liquid refrigerant form until it is full, therefore the dimensions of the accumulator should be carefully estimated during the design process. The inner volume of the accumulator was reduced to 1.5×10^{-3} m^3 in the next experiments. From Table 3 it could be found that after replacing the accumulator, the optimal R290 charge quantity is reduced to 1.3 kg, the cooling and heating capacity is much better, and the COP of rated refrigerating mode and heating mode, which is 2.8 and 3.27, respectively, is also slightly higher than the original. The Chinese national standards claimed that COP of a 13 kW ASHP which launched on the market should be not less than 2.5, the performance of this ASHP meet the relevant requirements.

Furthermore, the performance of this ASHP with 1.5×10^{-3} m^3 inner volume of the accumulator and 1.3 kg R290 charge quantity in the other conditions were also measured. In the high-temperature cooling condition, which the environment dry-bulb and water outlet temperature is 45 °C and 15 °C, respectively. The cooling capacity could reach 12.6 kW and the COP is 2.38. Then in the low-temperature heating condition, which the environment dry-bulb and water outlet temperature are −10 °C and 45 °C, respectively. The heating capacity is 8.5 kW, and the COP is 2.2. Hence, it could be obtained that the performance and the R290 charge quantity of this ASHP could comply with related standards. In the future, other technical methods such as using 5 mm diameter evaporator tube and optimize the structure of R290 scroll compressor it could be employed to further reduce the R290 charge quantity in the ASHP.

3. Risk assessment of the R290 ASHP

3.1. Experimental apparatus and procedures

The internal structure of this ASHP was illustrated in Fig. 3, its upper and lower parts are separated by the partition. The upper part contains the air-to-refrigerant heat exchanger and fan, and the R290 scroll compressor, plate-type heat exchanger, electronic expansion valve, four-way valve and ECC were involved in the lower part. In this study, the R290 will leak from the ASHP in different scenarios. The leakage of R290 was imitated by the Manifold Gauge Set (Fig. 2), one of its charging hoses was connected to the charge port of the ASHP, and another hose was acted as the leakage point and placed in the leak position (Fig. 3). The R290 in the ASHP will be released at the leak position by opening the stop valve of the manifold gauge set completely. As shown in Fig. 3, there are three different leakage positions to explore the impact of different leak positions. Leak position I was located in the lower part, it was fixed on the copper tube in front of the electronic expansion valve; leak position II and III was in the upper part, they were placed at the position of u-tube junctions of the air-to-refrigerant heat exchanger, which is the most likely leakage position recorded by service engineers. The leaked R290 gas will spread out from the ASHP through the ventilation grids on the bottom if the leakage occurs in the lower part, or through the fan outlet or air inlet while leakage occurs in the upper part.

In the actual situation, the ASHP is usually installed in the outdoor and the airflow will help to disperse the leakage gas. In this study, in order to eliminate the impact of airflow and accurately analyze R290 concentration in the surrounding area of the ASHP, the ASHP was placed in a wide room with an area over 50 m^2, and the window and door of the room will keep closed during the whole experimental process. Then, 9 infrared R290 gas detectors (A-I) with a range of 0–100% LFL were employed in this study to analyze the R290 concentration profiles near the ASHP, their arrangement locations in different scenarios will be described in detail below. Another 2 infrared R290 gas

Table 1
Specifications of the ASHP parameters.

Name	Specifications
Compressor	
Type	Scroll compressor (ZH13KCU)
Displacement	17.1 m^3/h
Oil quantity	1.9 L
Air cooled heat exchanger	
Type	Finned tube
Tube length (mm)	1315
Tube outer diameter (mm)	7.0
Tube inner diameter (mm)	6.56
Tube spacing (mm)	21.0
Number of tube row	2
Numbers of tubes	96
Inner volume (m^3)	4.2×10^{-3}
Heat transfer area (m^2)	50.4
Log mean temperature difference (°C)	8.5
Heat transfer coefficient (W/°C m^2)	42
Heat exchange capacity (kW)	17.99
Water side heat exchanger	
Type	Plate type
Inner volume (m^3)	0.6×10^{-3}
Heat transfer area (m^2)	0.97
Log mean temperature difference (°C)	5.0
Heat transfer coefficient (W/°C m^2)	3128
Heat exchange capacity (kW)	15.17

Fig. 1. Photograph of the heat pump performance measurement laboratory.

detectors (J, K) with a range of 0–100% VOL were utilized to measure the R290 concentration in the ECC, the measurement was carried out through an explosion-proof pump and some gas conduits. The explosion-proof pump drew the gas from the ECC into the measuring area of the infrared gas detector through the gas conduit, then sent it back to the ECC. The sampling site on the ECC was shown in Fig. 3 (the sampling site J and K). The R290 concentration data will be collected by the data acquisition instrument and recorded by the computer. The experimental instruments are detailed in Table 2, which were all fully calibrated. The LFL in this paper means the 2.1 vol%, and all gas detectors were calibrated by standard propane gas.

The R290 leakage experiments were carried out in the heating mode since it is the common mode of the heat pump, and the experimental procedures were carried out according to the following sequence:

(a) Ensure there is no residual R290 in the experimental room (the R290 concentration of background is less than 1.0% LFL).
(b) Connect the charging hose of the manifold gauge set to the charge port and install another hose on the leak position, charge the 1.3 kg R290 into the ASHP, then operate the ASHP into experimental conditions. The heating temperature is set at 45 °C.
(c) Start the data acquisition system, measuring and recording the R290 concentration in the experimental area. Shut down the ASHP once it reaches the experimental conditions and runs steadily for several minutes.
(d) Open the hand valve entirely on the manifold gauge set while the ASHP powered off, release the R290 at the leak position.
(e) Terminate the data acquisition system once all the concentration measurements drop to a very low value.

3.2. Scenario 1: The ASHP was placed away from the wall

Since the walls might hinder the spread of the R290, it needs to explore the impact of the distance between ASHP and wall on the safety of ASHP. In this scenario, the ASHP was placed away from the wall and the R290 was released at leak position I. The positions of the ASHP and the gas detectors were shown in Fig. 4. The ASHP was 2.0 m away from the two walls, and gas detectors A-I were put on the ground and near the ASHP to investigate the R290 concentration distribution in the ASHP surrounding area after the R290 leakage. The gas detectors A-D were placed on the front of the ASHP while E-H were on the back and I was on the side of the ASHP. The back of G and H was near to the wall and the distance between those two detectors and ASHP was 1.7 m, the gas detector G was on the axis of ASHP while H was on the right side and 0.5 m away from G. The gas detectors E and F were symmetrical about the axis of ASHP, 0.5 m apart from each other, and 0.85 m away from the ASHP. In addition, the gas detector I was parallel to the leak position I and 0.4 m away from the ASHP. Another gas detector J and K were employed to explore the R290 concentration in the ECC, the sampling site of them is revealed in Fig. 3. The photograph of this scenario was illustrated in Fig. 5.

The experiment was operated by following the experimental procedures, the results of the R290 concentration distribution on gas detectors A-I in this scenario are described in Fig. 6. The R290 concentration curve raised quickly at the beginning of the leakage, and several detectors reached and exceeded the LFL level. For the gas detectors A-I, the range of them is 0–100% LFL and the output data unit is 4–20 mA. If the R290 concentration exceed the LFL, the gas detectors will still output the maximum current signal (20 mA), so the curve in

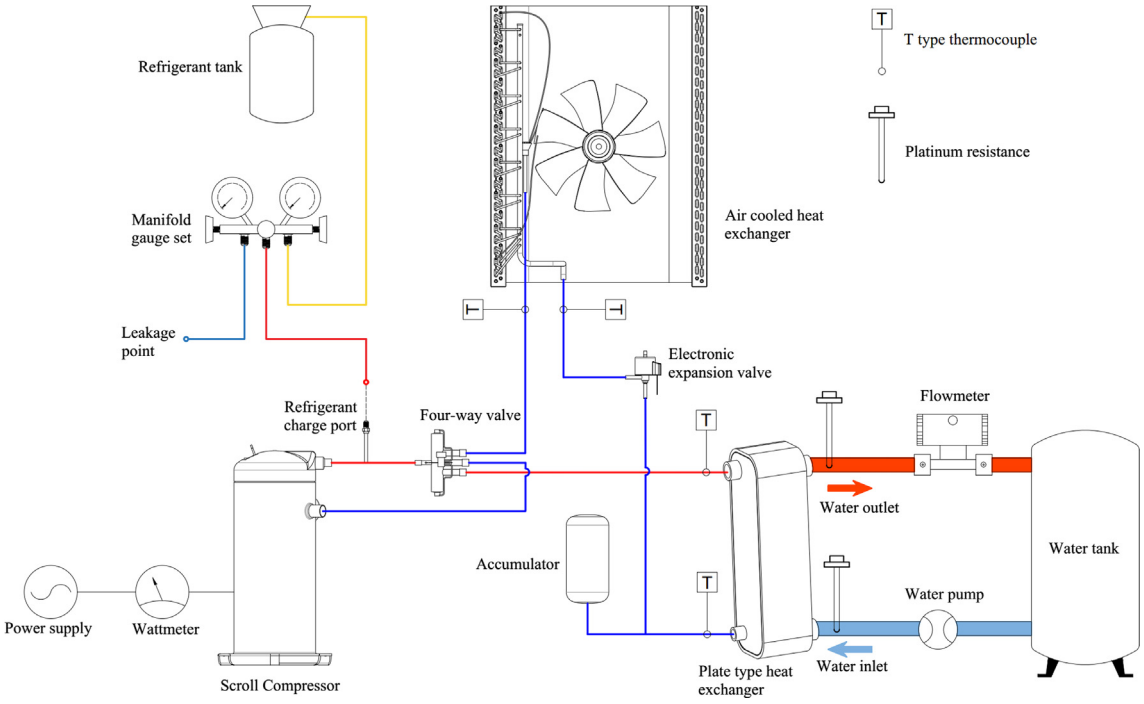

Fig. 2. Schematic of the performance experiment.

Table 2
Test apparatus specifications.

	Name	Type	Specifications
Performance experiment	Platinum resistances	INOR (66RKS type Pt 100)	Range: −50 to 120 °C; Accuracy Class: Class A
	T type thermocouples	OMEGA (5TC-TT-T-30)	Diameter: 0.25 mm; Accuracy: ± 0.1 °C
	Flowmeter	Coriolis Mass Flowmeter (DMF-1–4)	Range: 0–3000 kg/h Accuracy: ± 0.2% FS
	Wattmeter	8902F2	Range: 0–12 kW Accuracy: ± 0.2% FS
R290 leakage experiment	Infrared gas detectors (A–I)	Honeywell (Searchpoint optima plus)	Range: 0–100% LFL; Accuracy: ± 1% LFL
	Infrared gas detectors (J, K)	SKS-GA-C3H8	Range: 0–100 vol%; Accuracy: ± 1 vol%
	Data acquisition instrument	Agilent (34970A with 34901A module)	20 channels; Speed: 60 chs/s

Table 3
The performance of R290 ASHP in standard conditions.

	Cooling mode		Heating mode	
Environment dry-bulb temperature (°C)	35.0	35.0	7.0	7.0
Water outlet temperature (°C)	7.0	7.0	45.0	45.0
Evaporating temperature (°C)	1.0	1.2	−1.8	−2.2
Condensing temperature (°C)	49.6	48.7	49.7	50.2
Supercooling temperature (°C)	4.0	2.0	3.0	4.0
Inner volume of accumulator (m^{-3})	2.5	1.5	2.5	1.5
R290 charge quantity (kg)	1.8	1.3	1.8	1.3
Cooling/heating capacity (kW)	11.0	11.6	13.6	13.9
COP	2.62	2.8	3.25	3.27

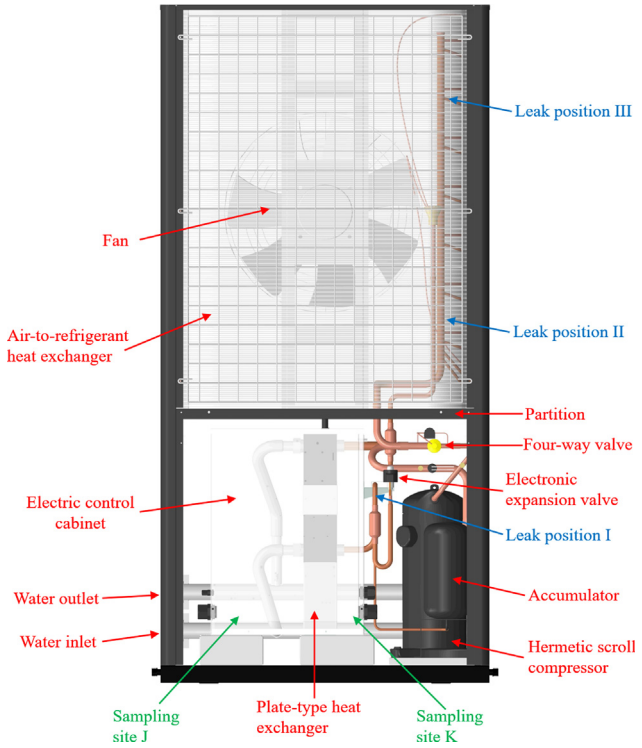

Fig. 3. The internal structure of the ASHP.

Fig. 6 is flat when the R290 concentration exceed the LFL, as the same with the following figures. Then the R290 concentration decreased gradually and stabilized as the R290 leakage rate decreased. In the beginning, the increase of the R290 concentration of the gas detector E-H (red lines) is prior to the A-D (black line) and I (green line). The gas detectors on the back (E-H) could respond to the refrigerant leakage faster because the leak position I is closer to the back of ASHP. However, the R290 concentration curve of A and B had an ascending process when E-H are declining, which could be inferred that the leaked R290 inside the ASHP might be more easily diffused from the ventilation grids on the front as the R290 leakage rate decreased. It could also be observed in Fig. 6 that the R290 concentration of the gas detector I first began to decrease and stabilized at the low value in the whole leakage process, then the R290 concentration of gas detectors E-H followed with I to decline but the trend was more gradual. It indicated that the side of the ASHP is the safest area during the leakage process since the R290 will diffuse out from the ventilation grids on the front and back of ASHP.

Comparing the results in the same side it could be found that the R290 concentration of gas detector C and D was higher than A and B, while E and F is higher than G and H. The R290 concentration was therefore related to the distance of the gas detectors to the ASHP, the shorter distance will result in the higher R290 concentration in the leakage process. Besides, the position of gas detector A–D and E–H were symmetrical about the ASHP as shown in Fig. 4. The results revealed that in the same distance, the R290 concentration of gas detectors on the front (C, D) is higher than the back (E, F) in the whole leakage process, A and B were lower than G and H in the beginning but will be higher in the later. Hence, the front of the ASHP is more dangerous than the back, and the position of gas detector C is the most hazardous of all gas detectors since it was located in the front and nearest to the leakage position. Fig. 6 also shown that the R290 concentration of gas detector C exceeded LFL level almost in the whole leakage process and the time was more than 1500 s. From the above, it can be concluded that the possibility of combustion in the ASHP surrounding area was related to the distance away from it, the area near the front is the most dangerous one and the combustible zone will appear in there more than 25 min.

3.3. Scenario 2: The ASHP was placed close to the wall

As a contrast, the ASHP was placed close to the wall in this scenario, the position of the ASHP and gas detectors were described as Fig. 7. The distance between the ASHP and the two walls was 0.6 m, which is the minimum distance specified in the operating manual. Gas detectors A–I were still placed on the ground, the relative position of gas detectors A–D and I to the ASHP were the same. The difference is that all of the gas detectors E–H were placed close to the wall, F and G were symmetrical about the axis of ASHP. The gas detector E was located on the left side of F, the distance between them was 0.5 m, and H was placed at the corner and 0.75 m apart from G. In this scenario, R290 was still released at the leak position I through the manifold gauge set.

Fig. 8 showed that the trend of the concentration curve is the same while ASHP was placed close to the wall: the R290 concentration raised quickly at the beginning, and the concentration of E–F (red lines) firstly increased. Then the concentration declined gradually as R290 leakage

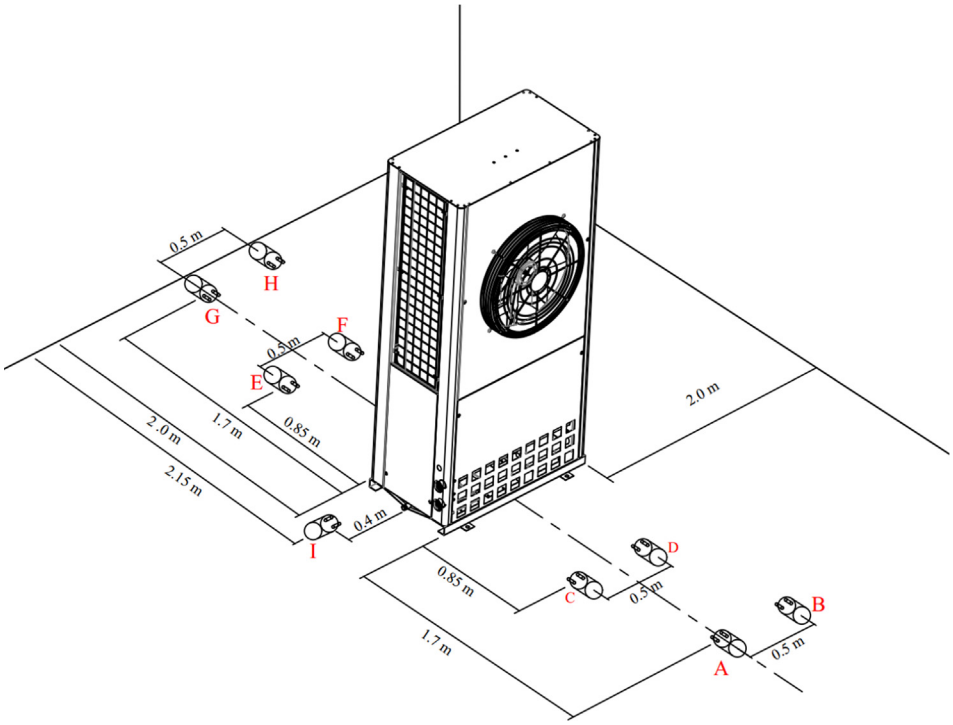

Fig. 4. Gas detectors layout when the ASHP was placed away from the wall.

rate decreased, and the gas detector I is still the first point began to decrease and stabilized at a low value. The gas detector C remained the most extended combustible zone's residence time, but the time in this scenario is over 1800 s, which is longer than the ASHP was placed away from the wall (1500 s). Besides, the concentration of all detectors will exceed LFL level for a long time (including gas detector A and B) in this scenario. It implied that the narrow space between the ASHP and the walls would make the area in front of the ASHP be more dangerous when the ASHP was placed close to the wall. Particularly, the R290 concentration of the gas detector H is much higher than others in the final, the walls might hinder the diffusion of R290 and gather the R290 gas in it since the gas detector H was placed at the corner. For the same reason, the R290 concentration of the gas detectors E–G is higher than that in the front of ASHP in the final. From these results we can infer that the position of the ASHP will affect its safety when the R290 leakage occurred. The combustible zone's residence time in the scenario that the ASHP was placed close to the wall will be 5 min longer than it was placed away from the wall. Hence, the ASHP should be installed away from the wall as far as possible in the actual condition.

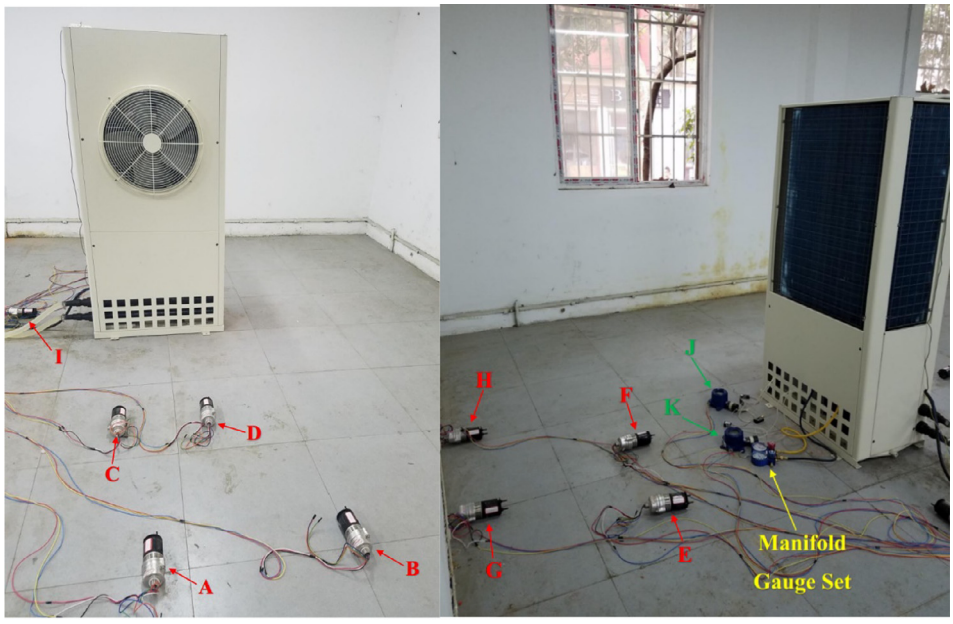

Fig. 5. Photograph of the ASHP and gas detectors while ASHP was placed away from the wall; front view (a) and back view (b).

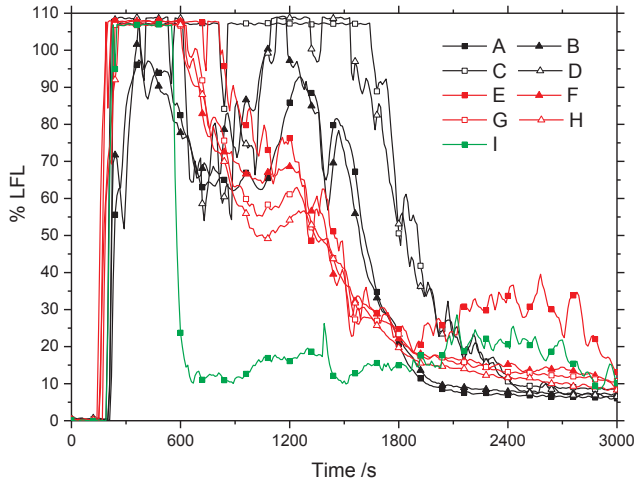

Fig. 6. R290 concentration distribution when the ASHP was placed away from the wall.

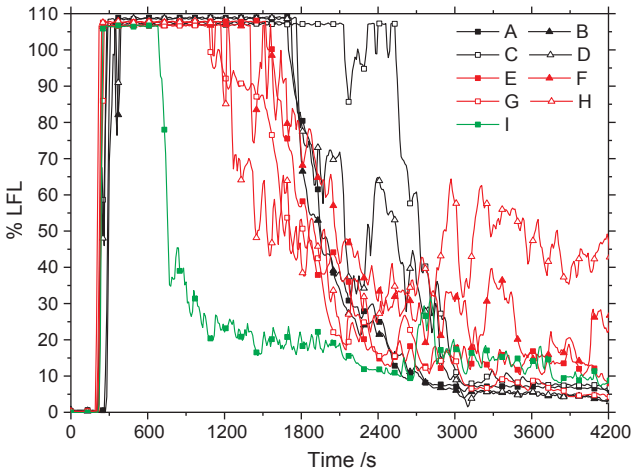

Fig. 8. R290 concentration distribution when the ASHP was placed close to the wall.

3.4. The R290 concentration inside the electric control cabinet

In the above results, the R290 concentrations in the area near the ASHP were presented. However, the R290 concentration inside the ASHP would be much higher than that of the outside when the R290 leakage accident occurred inside it. In this ASHP, the electrical components are concentrated in the ECC, any accident spark caused by short circuit appears in the ECC could lead to an internal fire of the ASHP. Thus, the R290 concentration in the ECC during the R290 leakage process was measured to analyze the possibility of combustion accident inside the ASHP, and the results were illustrated in Fig. 9.

The trend and duration time of the concentration curve in the ECC is similar to the outside region: the R290 concentration in the ECC raised quickly, then decreased gradually and stabilized. Fig. 9 showed that the R290 concentration starts to decrease at the moment when 300 s after the leakage occurs. It could also be found in Figs. 6 and 8 that the leakage occurred at the 300 s, and the R290 concentration of the gas detector I decreased at the 600 s. The R290 leakage rate might be too slow to maintain the R290 concentration keep increasing. Likewise, the duration time of the whole leakage process in Fig. 9 is about 1500 s when the ASHP was placed away from the wall, and 1800 s when the ASHP was close to the wall, which is also similar to the results as shown in Figs. 6 and 8. Furthermore, the concentration of gas detector K is always higher than J since the sampling site K is closer to the leak position I according to the Fig. 3. The R290 concentration of gas detector J and K is much higher in the scenario that the ASHP was placed close to the wall than that away from the wall. The fire hazard might increase not only in the surrounding area but also in the inner space if the ASHP was placed close to the wall.

It is noteworthy that whether ASHP was placed close or away from the wall, the R290 concentration in the ECC will exceed the LFL level (2.1 vol%), and remain at a high value in the final. The final R290 concentration even exceeded the LFL level when the ASHP was placed close to the wall. By contrast, the R290 concentration in the region near the ASHP is very low after 3000 s according to Figs. 6 and 8. This phenomenon might be related to the insufficiently ventilated inside the

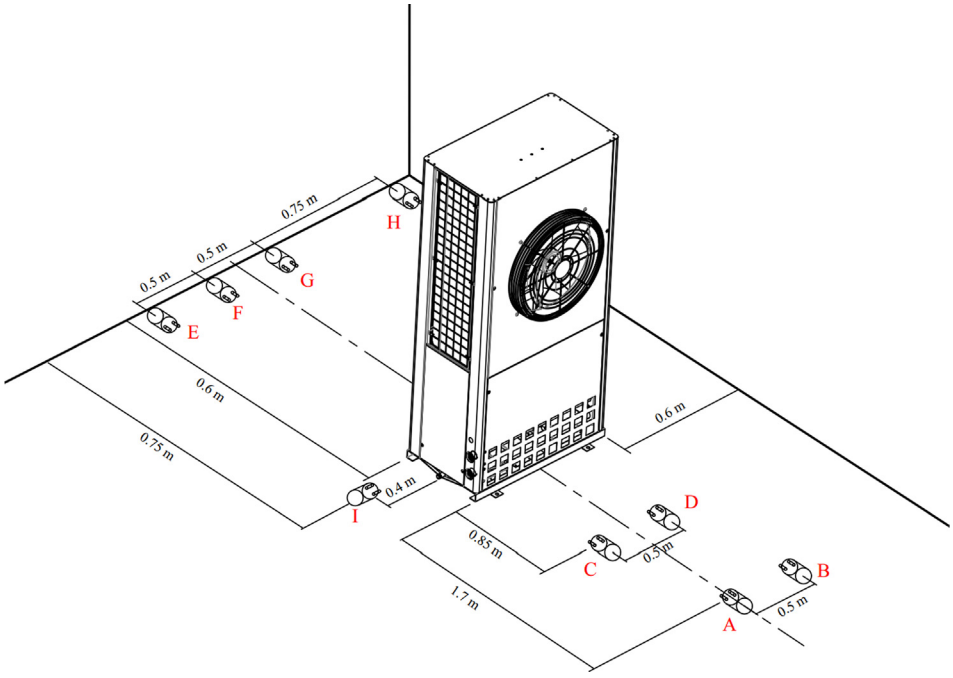

Fig. 7. Gas detectors layout when the ASHP was placed close to the wall.

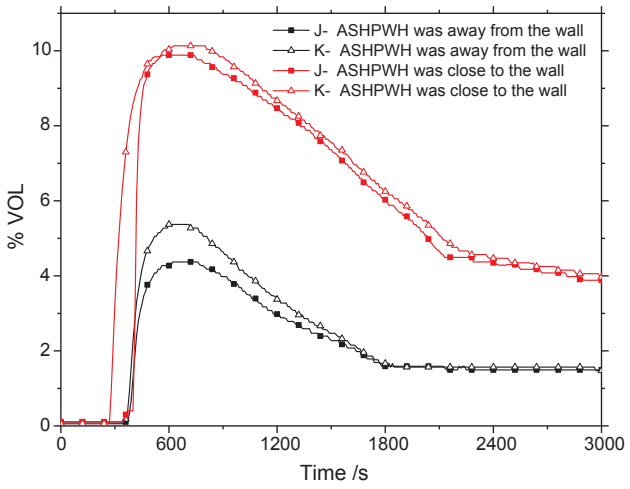
J- ASHPWH was away from the wall
K- ASHPWH was away from the wall
J- ASHPWH was close to the wall
K- ASHPWH was close to the wall
% VOL
Time /s

Fig. 9. R290 concentration distribution in the electric control cabinet of the ASHP.

ECC, once the R290 get into the in the ECC, the gas can hardly diffuse out and would gather in it. Hence, the ECC needs to take some safety measures to improve the ventilation and guarantees that the fire risk will not appear in it.

3.5. Scenario 3: Measurement of the R290 concentration in the region away from the ground

In the previous experiments, the R290 concentration distribution results were carried out in the situation that all gas detectors were put on the ground. In order to measure the R290 concentration distribution in the region near the ASHP and away from the ground, another experiment was carried out and the gas detectors layout was shown in Fig. 10. The ASHP was still close to the walls to imitate the most dangerous situation, and the gas detectors A-H were placed in the front of the ASHP since the R290 concentration in the front is higher than in the back according to the previous results. The gas detector I was still on the side and 0.4 m away from the ASHP, but it was parallel to the front of the ASHP, not the leak position as previous. The gas detectors A and B were 2.0 m away from the ASHP while C–H were 1.0 m away from it, all of them were symmetrical about the axis of ASHP and the distance between each other was 0.8 m, which is equal to the width of the ventilation grids. The gas detectors A and B were on the ground, the height of C and D was 0.1 m while E and F was 0.5 m, and G and H were 0.7 m away from the ground, which is the same height with the partition of ASHP. The R290 concentration inside the ECC will always exceed the LFL level according to the previous results, the gas detectors J and K were therefore not employed in this experiment.

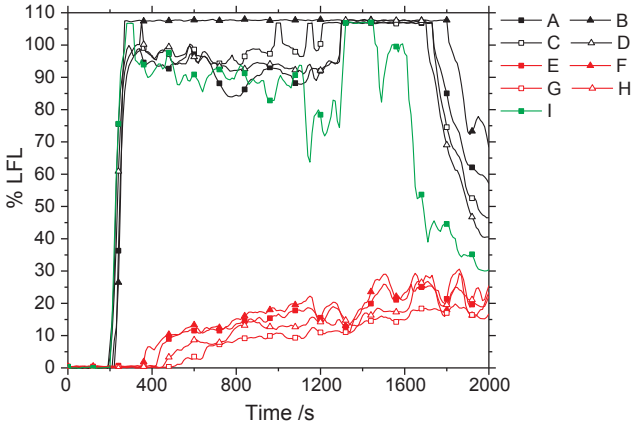

Fig. 11. R290 concentration distribution in the area away from the ground.

The results of R290 concentration distribution in the region away from the ground were shown in Fig. 11. It could be clearly found in Fig. 11 that the R290 concentration of gas detector E–H remained at a

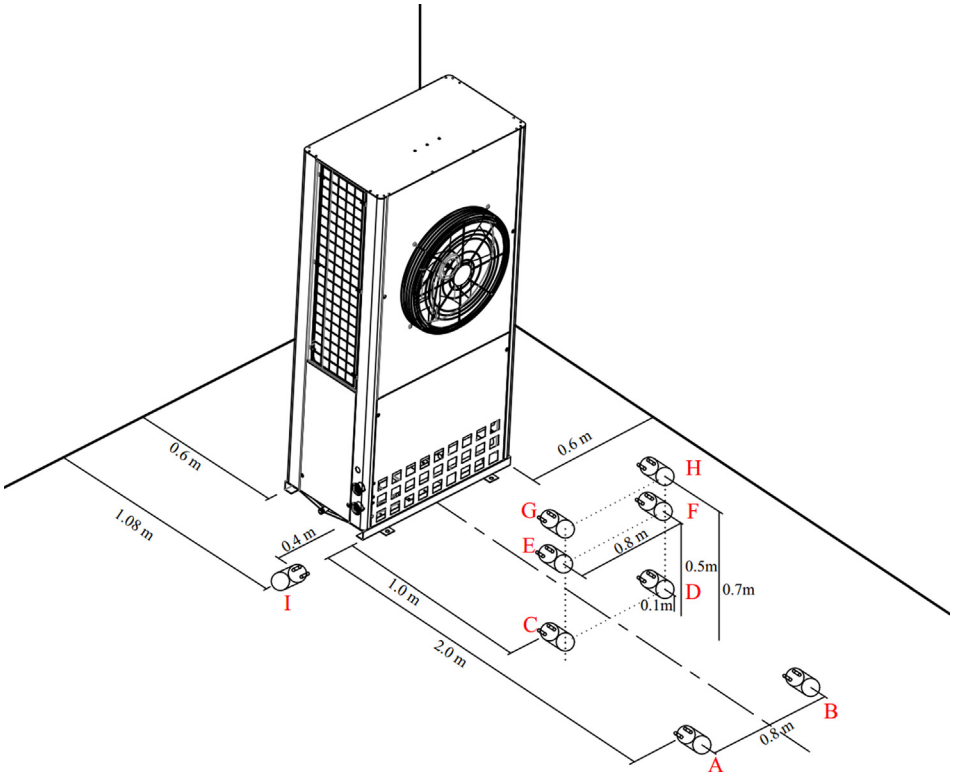

Fig. 10. Gas detectors layout when measuring the R290 concentration distribution in the region away from the ground.

low value during the whole leakage process, the R290 concentration of detector C is not the highest since it was not put on the ground but on the height of 0.1 m. The gas detector B was placed on the floor in front of the ASHP, so it has the highest R290 concentration and longest combustible zone's residence time. Likewise, the gas detector I was placed in the position where was closer to the front of the ASHP than the previous, the R290 concentration of it was therefore higher. It is evident that the curve of R290 concentration of gas detectors E–H (red lines) in the Fig. 11 is much lower than the LFL level, the position of these gas detectors was at least 0.5 m away from the ground as shown in Fig. 10. As a contrast, the gas detectors A–D and I were placed on the ground or near the ground, so the R290 concentration of them could exceed the LFL in the leakage process. From these results it could be concluded that the fire risk region will only appear near the floor while the R290 leakage occurs inside the ASHP.

3.6. Scenario 4: R290 leaked from the upper part

In the actual situation, the R290 leakage could also occur in the upper part. For example, once the unqualified welding exists on the u-tube junctions of the air-to-refrigerant heat exchanger, it could lead to an R290 leakage in the upper part. Hence, the experiments of R290 leaked from the ASHP upper part were also carried out. The leak position II and III were located at the position of u-tube junctions of the air-to-refrigerant heat exchanger, 0.75 and 0.25 m away from the top of the ASHP, respectively. The ASHP and gas detectors layout when R290 leakage occurred in the upper part of the ASHP was shown in Fig. 12, the ASHP was still placed close to the wall. The gas detectors A-D were placed at the front of the ASHP, A and B were on the ground and symmetrical about the axis of ASHP, they were 2.0 m away from ASHP and 0.8 m apart from each other; The gas detectors C and D were placed at the axis of ASHP and 1.0 m away from the ASHP, the height of D was 0.1 m, and the height of both C and the bottom of the fan outlet was 1.0 m. The gas detectors E–I were placed on the side of ASHP, E and F were parallel to the front of ASHP while G and H were 0.6 m apart from them, the distance from the gas detectors E-H to the ASHP was 1.0 m. The heights of gas detector F and H were 0.1 m while E and G were 0.6 m, which is the same with the bottom of the air-to-refrigerant heat exchanger; the gas detector I was on the ground and parallel to the center of the ASHP, 2.0 m apart from the ASHP. In addition, the gas

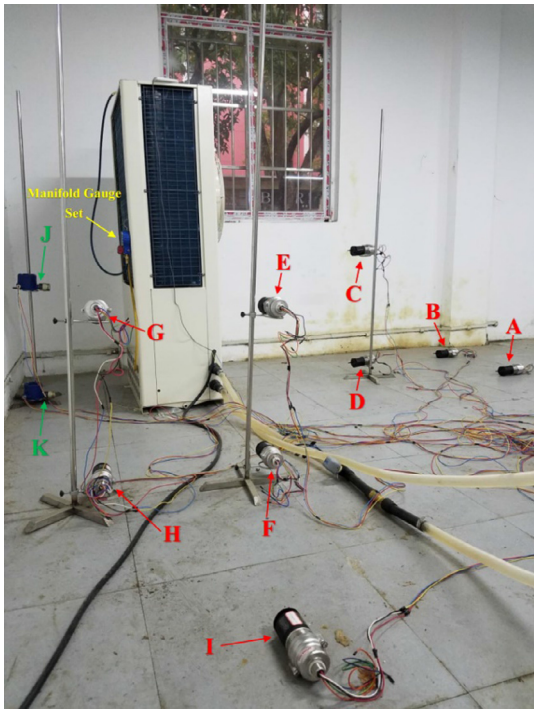

Fig. 13. Photograph of the gas detectors and the ASHP when R290 leakage occurred in the upper part of the ASHP.

detectors J and K were located at the back of ASHP to measure the maximum R290 concentration in the back, they were placed at the axis of ASHP and near the wall, the height of J and K were 0.6 and 0.1 m, respectively. Fig. 13 is the photograph of the gas detectors and the ASHP while R290 leakage occurred in the upper part of the ASHP.

The R290 concentration distribution of the gas detectors A-I while R290 leakage occurred in leak position II and III were described in Figs. 14 and 15. In these two scenarios, the gas detectors C, E and G were placed away from the ground, the R290 concentration of these three detectors therefore remain at a low value in the whole leaking process whether the R290 released at leak position II or III. Besides, the

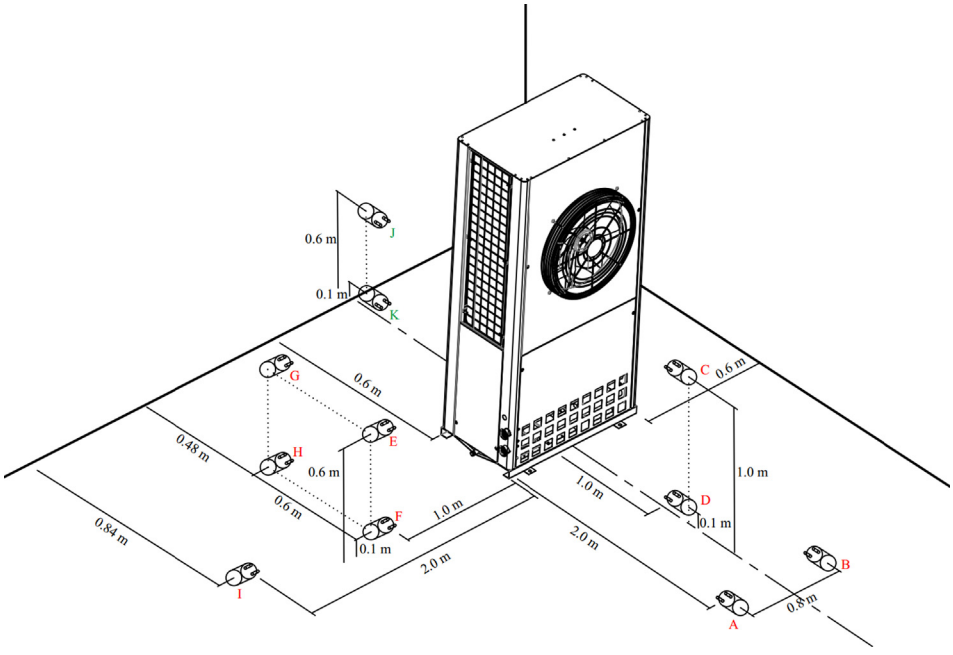

Fig. 12. Gas detectors layout when R290 leakage occurred in the upper part of the ASHP.

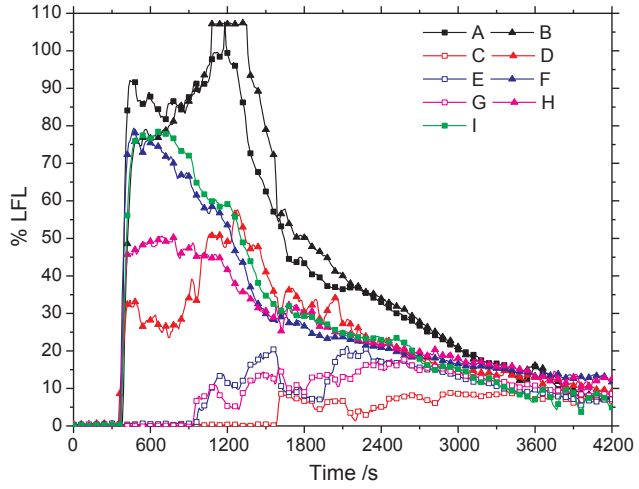

Fig. 14. R290 concentration distribution when R290 leaked at leak position II.

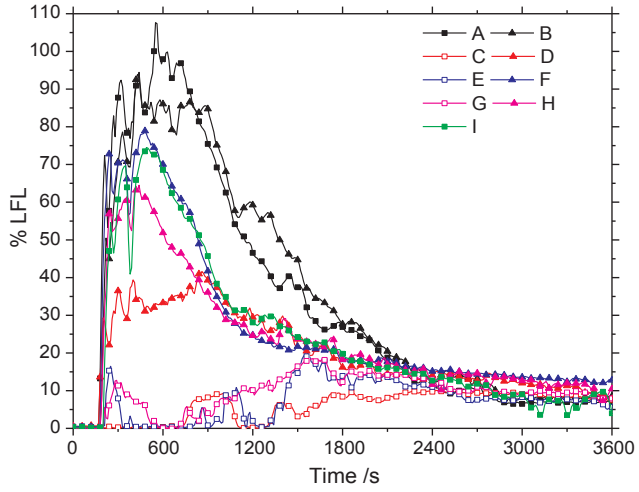

Fig. 15. R290 concentration distribution when R290 leaked at leak position III.

R290 concentration of the gas detector C is the lowest because of its highest position. By comparing these two results with the previous, it could be found that the number of gas detectors which its concentration exceeds the LFL level is significantly reduced when the R290 leaked from the air-to-refrigerant heat exchanger. Fig. 14 illustrates that only the gas detector A and B could reach the LFL level and the combustible zone's residence time is shortened to about 300 s when R290 released at leak position II. In addition, the fire risk region only appears in the gas detector A and the combustible zone's residence time is just about tens of seconds as shown in Fig. 15. The risk around the ASHP was also related to the height of the leakage position. Furthermore, the R290 concentration of gas detectors D is lower than F and H in the leakage process. Since all of them were mounted at the height of 0.1 m, it might be due to that the height of the fan outlet is higher than the air inlet of the air-to-refrigerant heat exchanger.

The R290 concentration of the gas detector J and K were illustrated in Fig. 16, the results were similar with the gas detectors A–I: The R290 concentration of the gas detector J remain at a low value in the leakage process since it was placed away from the ground. The R290 concentration of the gas detector K when R290 released at leak position II is higher and could exceed the LFL level because the leak position II is lower. It could be concluded that when R290 leaked at a higher position, the safety condition around the ASHP is much better: the fire hazard still only appeared near the ground, but the combustible zone is shrunk and its residence time is shortened.

4. Conclusions and suggestions

This paper conducted various experiments about the performance of R290 in a 13 kW ASHP and the risk assessment of the R290 ASHP. Based on the experimental results, the main conclusions of the present study and suggestions for improving the design of the R290 ASHP to minimize the risk are as follows:

(1) R290 has an excellent heating performance in the ASHP. Within the allowable refrigerant charge quantity of EN 378, the COP of this 13 kW R290 ASHP with 1.3 kg charge quantity could reach 2.8 and 3.27 in the rated refrigerating and heating conditions. In order to reduce the refrigerant charge quantity in the ASHP, the diameter of the tube of air-to-refrigerant heat exchanger could be reduced and the high efficiency plate-type heat exchanger could be utilized. The inner volume of the accumulator needs to match the heat capacity of the plate-type heat exchanger.

(2) The distance between the ASHP and the walls could affect the safety of the R290 ASHP. The closer the distance is, the more dangerous the ASHP will be when an R290 leakage occurs in it. The ASHP should therefore install as far away from the walls as possible within the requirements of the operating manual.

(3) In the conditions of this study, the R290 concentration approaches or exceeds the LFL only appeared in the region where around the ASHP and extremely close to the ground. The R290 concentration can hardly exceed LFL at the height of 0.1 m, and it is much lower than the LFL in the area with a height exceeding 0.5 m. The power supply of the R290 ASHP should be installed away from the ground, and the hazard marking and signage need to be used around the ASHP to warning the technicians that the refrigerant in the ASHP is flammable.

(4) The height of leak position has a significant influence on the safety of the area around the ASHP. The lower leak position results in a more expansive combustible zone and longer residence time around the ASHP. The combustible zone will appear near the ASHP in the whole leakage process when the R290 leakage occurs in the lower part. Conversely, the combustible zone will be shrunk and its residence time will be shortened when R290 leakage occurs in the upper part. The quality inspection in the lower part of the ASHP needs to be more careful to ensure that unqualified welding will not exist in it.

(5) Once the R290 gas enters into the ECC, it will be hard to diffuse out. In certain scenarios, the R290 concentration inside the ECC could exceed the LFL level even after the leakage is over. The design

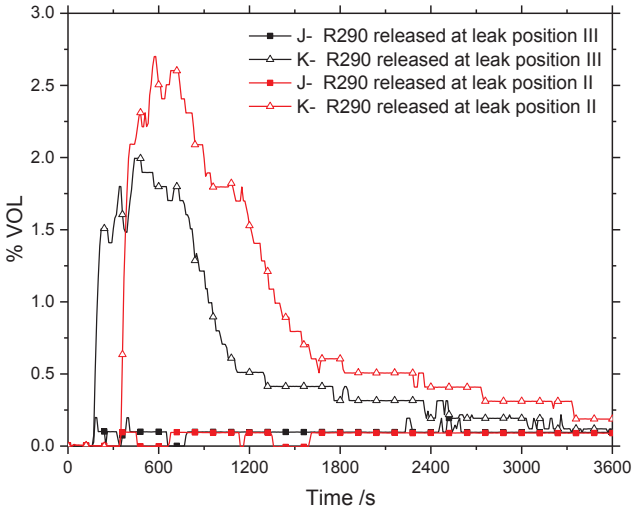
J- R290 released at leak position III
K- R290 released at leak position III
J- R290 released at leak position II
K- R290 released at leak position II
% VOL
Time /s

Fig. 16. R290 concentration distribution of gas detector J and K.

position of the electronic control cabinet should be kept away from the refrigerant system. Besides, the face of the ECC facing the refrigerant system should be welding sealed, the door of the ECC should face towards to the outside of the ASHP and be sealed by the gasket, the inlet and outlet of the electric wires from the ECC also need to be sealed by the soft rubber. Other safety measures, such as add some ventilation grids at the bottom of the ASHP could also consider to be employed to enhance the air convection in the lower part of the ASHP and guarantee the R290 gas will not gather in it.

Since the researches about the safety of R290 leakage was mainly concentrated on the air conditioner and there is no literature available about the R290 ASHP, the results presented in this study could be considered as a preliminary guideline for the refrigeration field. The research about the safety of the R290 ASHP is still need to deeply studied.

References

[1] F. Ju, X. Fan, Y. Chen, H. Zhang, T. Wang, X. Tang, Performance assessment of heat pump water heaters with R1233zd(E)/HCs binary mixtures, Appl. Therm. Eng. 123 (2017) 1345–1355.

[2] Z. Li, P. Bie, Z. Wang, Z. Zhang, H. Jiang, W. Xu, J. Zhang, J. Hu, Estimated HCFC-22 emissions for 1990–2050 in China and the increasing contribution to global emissions, Atmos. Environ. 132 (2016) 77–84.

[3] Z. Yang, X. Wu, Retrofits and options for the alternatives to HCFC-22, Energy 59 (2013) 1–21.

[4] L. Höglund-Isaksson, P. Purohit, M. Amann, I. Bertok, P. Rafaj, W. Schöpp, J. Borken-Kleefeld, Cost estimates of the Kigali Amendment to phase-down hydrofluorocarbons, Environ. Sci. Policy 75 (2017) 138–147.

[5] J. Blanco Castro, J.F. Urchueguía, J.M. Corberán, J. Gonzálvez, Optimized design of a heat exchanger for an air-to-water reversible heat pump working with propane (R290) as refrigerant: modelling analysis and experimental observations, Appl. Therm. Eng. 25 (2005) 2450–2462.

[6] Y.S. Chang, M.S. Kim, S.T. Ro, Performance and heat transfer characteristics of hydrocarbon refrigerants in a heat pump system, Int. J. Refrig. 23 (2000) 232–242.

[7] K. Nawaz, B. Shen, A. Elatar, V. Baxter, O. Abdelaziz, R290 (propane) and R600a (isobutane) as natural refrigerants for residential heat pump water heaters, Appl. Therm. Eng. 127 (2017) 870–883.

[8] P. Fernando, B. Palm, P. Lundqvist, E. Granryd, Propane heat pump with low refrigerant charge: design and laboratory tests, Int. J. Refrig. 27 (2004) 761–773.

[9] R. Ghoubali, P. Byrne, F. Bazantay, Refrigerant charge optimisation for propane heat pump water heaters, Int. J. Refrig. 76 (2017) 230–244.

[10] R.K. Eckhoff, M. Ngo, W. Olsen, On the minimum ignition energy (MIE) for propane/air, J. Hazard. Mater. 175 (2010) 293–297.

[11] J.M. Kuchta, Investigation of Fire and Explosion Accidents in the Chemical, Mining, and Fuel-Related Industries: A Manual, Technical Report Archive & Image Library, 680, 1986.

[12] J.M. Corberán, J. Segurado, D. Colbourne, J. Gonzálvez, Review of standards for the use of hydrocarbon refrigerants in A/C, heat pump and refrigeration equipment, Int. J. Refrig. 31 (2008) 748–756.

[13] D. Colbourne, K.O. Suen, Appraising the flammability hazards of hydrocarbon refrigerants using quantitative risk assessment model Part I: modelling approach, Int. J. Refrig. 27 (2004) 774–783.

[14] D. Colbourne, L. Espersen, Quantitative risk assessment of R290 in ice cream cabinets, Int. J. Refrig. 36 (2013) 1208–1219.

[15] D. Colbourne, K.O. Suen, Comparative evaluation of risk of a split air conditioner and refrigerator using hydrocarbon refrigerants, Int. J. Refrig. 59 (2015) 295–303.

[16] A. Gigiel, Safety testing of domestic refrigerators using flammable refrigerants, Int. J. Refrig. 27 (2004) 621–628.

[17] L. Jia, W. Jin, Y. Zhang, Experimental study on R32 leakage and diffusion characteristic of wall-mounted air conditioners under different operating conditions, Appl. Energy 185 (Part 2) (2017) 2127–2133.

[18] T. Li, Indoor leakage test for safety of R-290 split type room air conditioner, Int. J. Refrig. 40 (2014) 380–389.

[19] W. Zhang, Z. Yang, J. Li, C.-X. Ren, D. Lv, J. Wang, X. Zhang, W. Wu, Research on the flammability hazards of an air conditioner using refrigerant R-290, Int. J. Refrig. 36 (2013) 1483–1494.

[20] W. Zhang, Z. Yang, X. Zhang, D. Lv, N. Jiang, Experimental research on the explosion characteristics in the indoor and outdoor units of a split air conditioner using the R290 refrigerant, Int. J. Refrig. 67 (2016) 408–417.

[21] B. Palm, Refrigeration systems with minimum charge of refrigerant, Appl. Therm. Eng. 27 (2007) 1693–1701.

[22] J.M. Corberán, I.O. Martínez, J. Gonzálvez, Charge optimisation study of a reversible water-to-water propane heat pump, Int. J. Refrig. 31 (2008) 716–726.

[23] A. Cavallini, E. Da Riva, D. Del Col, Performance of a large capacity propane heat pump with low charge heat exchangers, Int. J. Refrig. 33 (2010) 242–250.

[24] IIR, Refrigerant Charge Reduction in Refrigerating Systems, International Institute of Refrigeration, 25th Informatory Note on Refrigeration Technologies, 2014.

[25] J. Gao, G. Ding, T. Wang, Y. Gao, J. Song, Optimal design principle for air conditioner with refrigerant R290, Chinese J. Refrig. Technol. 33 (2013) 23–26.

[26] S. Cheng, S. Wang, Z. Liu, Cycle performance of alternative refrigerants for domestic air-conditioning system based on a small finned tube heat exchanger, Appl. Therm. Eng. 64 (2014) 83–92.

[27] G.A. Longo, S. Mancin, G. Righetti, C. Zilio, Hydrocarbon refrigerants HC290 (Propane) and HC1270 (Propylene) low GWP long-term substitutes for HFC404A: a comparative analysis in vaporisation inside a small-diameter horizontal smooth tube, Appl. Therm. Eng. 124 (2017) 707–715.